Bulletin of Electrical Engineering and Informatics
Vol. 14, No. 6, December 2025, pp. 4482~4494
ISSN: 2302-9285, DOI: 10.11591/eei.v14i6.10742

Brain tumor classification using PCA-NGIST features with an enhanced RELM classifier

Bukkapatnam Rakesh Babu[1], Vullanki Rajesh[1], Bodapati Venkata Rajanna[2], Shaik Hasane Ahammad[1]
[1]Department of Electronics and Communication Engineering, Koneru Lakshmaiah Education Foundation, Guntur, India
[2]Department of Electrical and Electronics Engineering, MLR Institute of Technology, Hyderabad, India

Article Info

Article history:

Received May 23, 2025
Revised Aug 28, 2025
Accepted Sep 27, 2025

Keywords:

Brain tumour
Brain tumour classification
Enhanced RELM classifier
Magnetic resonance imaging
PCA-NGIST

ABSTRACT

Brain tumours may cause severe health risks because of abnormal cell growth, which may result in organ malfunctions and death in adulthood. As precise identification of the tumour type is required for effective treatment. Magnetic resonance imaging (MRI) has recently been provided as an effective method for brain tumour diagnosis by computer-based based systems. To categorize brain tumours from MRI images, the paper offered a fusion model integrating an enhanced regularized extreme learning machine (RELM) classifier with principal component analysis (PCA) and normalized GIST (NGIST) feature extraction. While NGIST extracts strong spatial and texture features essential for modelling the tumour, PCA reduces the dimension of the input features without sacrificing significant data patterns. The improved RELM efficiently categorizes brain tumours into three categories: pituitary, meningioma, and glioma. It is optimized to improve learning capacity and generalization. The novelty of this study lies in the integration of NGIST descriptors with PCA-driven dimensionality reduction and an enhanced RELM classifier in a single lightweight framework. Unlike conventional methods that trade accuracy for computational cost, the proposed model ensures high precision and recall while remaining computationally efficient. This unique fusion demonstrates significant improvements in both diagnostic accuracy of 96% and clinical applicability, offering a balanced solution for real-time brain tumor classification.

Corresponding Author:

Bodapati Venkata Rajanna
Department of Electrical and Electronics Engineering, MLR Institute of Technology
Hyderabad, India
Email: rajannabv2012@gmail.com

1. INTRODUCTION

Abnormalities of the brain that are frequently referred to as tumours in medical field. Approximately 200 distinct kinds of brain tumours can develop in different locations of the human brain. These tumours have the potential to significantly and frequently influence a person's life. Comprehensive scientific proof of rising brain tumor occurrence and its correlation with death among people is provided by numerous studies [1]. The American Cancer Society states that brain tumours are one of the dangerous conditions where the brain's tissues grow peculiarly and damage brain function. According to the National Brain Tumour Foundation's research, over the previous three decades, the number of persons who have died from brain tumours has climbed by 300% [2]. Brain tumors have emerged as the world's most significant difficulty and are among the deadliest medical conditions. Brain tumors in both adults and children are uniform, according to another analysis of cancer signs [3]. In another report, about 80,000 new instances of primary brain tumors

36.3% of cases were meningioma, 26.5% were gliomas, and approximately 16.2% were pituitary tumors [4]. The remaining instances were of other brain tumor kinds, including malignant, medulloblastoma, and lymphomas [5]. It can be difficult for medical professionals to detect and provide prompt treatment for patients due to the physical characteristics of the brain and the complexity of brain tumours. Enhancing the survival number of patients with brain tumours requires early detection and appropriate treatment. Proper classification and early diagnosis are critical to improving patient outcomes via proper treatment [6].

The optimal selection and most commonly employed method of diagnosing brain tumours is magnetic resonance imaging (MRI) [7]. High-resolution images of the internal structure of the brain are offered by MRI, which is critical for identifying tumors in the brain. It assists practitioners in identifying and classifying tumors. Different MRI modalities are generated for various types of brain tumor identification and provide essential structural information for brain tumor classifying and identification and their regions [8], [9] achieved 92.31% accuracy with a cost-sensitive deep neural network (DNN) but struggled with unbalanced datasets; [10] reported 93% with artificial neural network (ANN) though results varied with MRI parameters; [11] obtained 94% using convolutional neural network (CNN) but faced overfitting on small data; [12] reached a mean dice score of 89.78% with a CNN–hypercolumn method but only 67.90% in survival prediction; [13] achieved 91.9% with K-means and ANN though manual feature extraction risked missing details. Overall, deep models demand large, balanced datasets and high computational cost, while traditional methods lack spatial-texture capture. Hybrid CNN–texture approaches improves feature richness but often lack interpretability. A comparative overview of related works and our proposed framework is provided in the paper. Prior principal component analysis-generalized search tree (PCA–GIST) hybrids struggle with intensity variations, and conventional regularized extreme learning machine (RELM) classifiers face overfitting and poor generalization, whereas our framework integrates NGIST with PCA-driven dimensionality reduction and enhanced RELM to overcome these issues. The novelty lies in NGIST normalization for stable MRI feature extraction and Enhanced RELM with Tikhonov regularization for balanced generalization and efficiency, setting our approach apart from conventional PCA–GIST or RELM methods.

The primary aspects of our proposed study can be brought up as follows:

- In the first phase, we use the image normalization technique to normalize the MRI picture to guarantee consistent input values, reducing the influence of noise andimage intensity changes in the stage of preprocessing.
- We employed NGIST multi-scale Gabor filters to capture both texture and spatial data. By keeping the most pertinent information throughout the feature extraction phase, PCA lowers the feature dimensions for more effective categorization.
- We use enhanced RELM classifier and it is a single-layered, fastest neural network-based model. Regularization is used to prevent overfitting. Features from several tumour kinds are used to train the classifier. Using traits that have been retrieved, the enhanced RELM predicts the kind of tumour during testing.
- Finally, the tumour is classified as either pituitary, glioma, or meningioma based on the classifier's output.

The following sections make up the framework of the paper. In section 2, the proposed work is presented. The experimental results of the proposed methods, implementation details, and a comparison with other current techniques are all included in section 3. In section 4 conclusion of the work is summarized.

2. PROPOSED WORK

In this particular section, we detail the proposed methodology, the block diagram representation of proposed work is shown in the Figure 1. The flowchart of enhanced RELM architecture is shown in Figure 2.

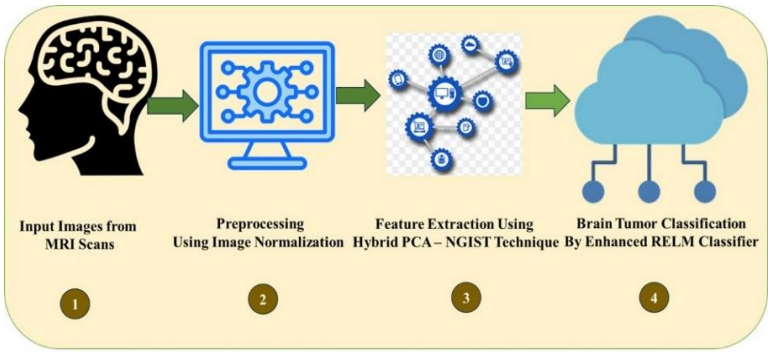

Figure 1. Block diagram of the proposed framework for brain tumor classification

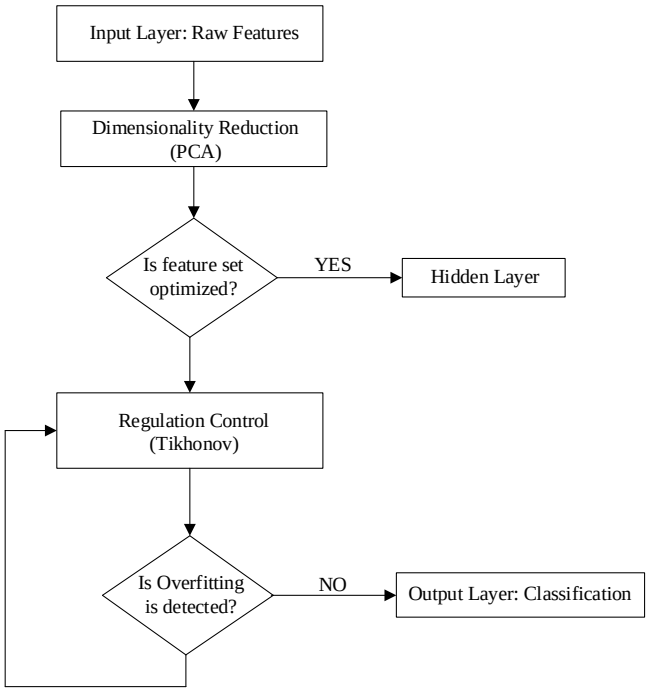

Figure 2. Flowchart of enhanced RELM architecture

2.1. Preprocessing of brain images

Preprocessing is essential in medical imaging to standardize MRI scans, reduce noise, and address acquisition variations, thereby improving accuracy and reliability [14]. MRI images are converted from 256×256 pixels into one-dimensional arrays for computational efficiency and compatibility with machine learning models [15]. Brightness and contrast are equalized by uniformly scaling pixel intensities, and normalization as shown in (1). The preprocessing pipeline applies intensity normalization, skull stripping, and Gabor-based artifact removal to standardize scans, eliminate non-brain tissues, and enhance edge clarity, preserving only relevant brain structures for feature extraction. Figure 3 illustrates preprocessing results: Figure 3(a) shows the original MRI brain input, while Figure 3(b) displays the normalized MRI image after preprocessing.

$$Normalised\ value = \frac{pixel\ value - Min\ value}{Max\ value - Min\ value} \quad (1)$$

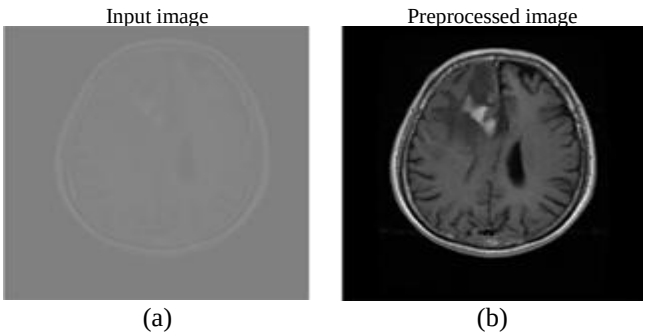

Figure 3. Preprocessing results in; (a) example of an image brain input image and (b) preprocessed MRI image after normalization

A prefiltering stage with multi-orientation Gabor filters was applied after normalization to reduce noise and enhance structural details in MRI scans. This minimized irrelevant textures, enabling NGIST to capture stronger tumor-specific features.

2.2. Extracting brain features using hybrid PCA-NGIST approach

Feature extraction distinguishes tumor types in MRI images, essential for brain tumor classification. The hybrid method integrates PCA for dimensionality reduction with NGIST for feature extraction, ensuring efficient and cost-effective classification.

2.2.1. NGIST feature extraction

Spatial and orientation-specific information is derived from the input MRI image through the application of the GIST descriptor [16]. To facilitate the extraction of texture patterns that encapsulate diverse cellular architectures, Gabor filters, which respond to specific edges and orientations, are employed at multiple scales. The input MRI image has been standardized to a resolution of 256×256 pixels to ensure consistency across all imaging assessments. Prefiltering is used to minimize noise prior to feature extraction, improving the clarity of significant textures. Figure 4 shows prefiltered MRI images with noise reduction and texture enhancement: Figure 4(a) corresponds to glioma, Figure 4(b) meningioma, and Figure 4(c) pituitary tumors.

(a) (b) (c)

Figure 4. Prefiltered MRI images illustrating noise reduction and texture enhancement; (a) glioma, (b) meningioma, and (c) pituitary brain tumours

The representation of the Gabor filter dictionary, which illustrates how different filters react to different orientations, improves the extraction of important texture information and demonstrates the model's ability to capture important image qualities. As well, Figure 5 shows images of brain tumour feature extraction, demonstrating the model's capacity to preserve crucial spatial information. The enhanced RELM classifier can distinguish between minute changes in tumour structure thank to this method's extensive feature set, which enhances classification performance.

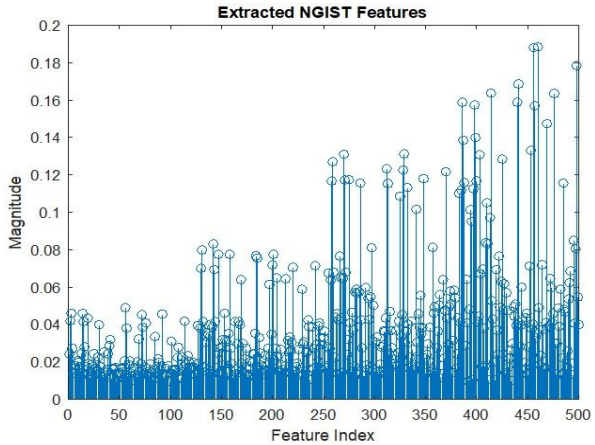

Figure 5. NGIST feature extracted tumours from dataset

2.2.2. Dimensionality reduction using principal component analysis

PCA reduces the dimensionality of extracted NGIST features by selecting the most relevant components, minimizing redundancy and computational load while retaining crucial details for accurate classification [17]. The training dataset combines NGIST features from MRI scans of pituitary, glioma, and

meningioma tumours. The number of hidden neurons (1500) in enhanced RELM was determined experimentally to balance accuracy and training speed. The regularization parameter λ was fixed at 1e−10, as this value consistently minimized overfitting across validation runs. PCA components were selected to retain ≥95% variance, ensuring compact yet informative features. Compared to standard GIST, NGIST incorporates normalization of feature vectors, which reduces sensitivity to illumination and intensity variations, thereby improving robustness in MRI-based tumor classification.

2.3. Classifying brain tumours

The framework's final phase classifies brain tumors using features extracted by PCA–NGIST. This is achieved with an enhanced RELM, a fast-learning neural network employing Tikhonov regularization to improve generalization and prevent overfitting [18]. The classification process involves multiple stages.

2.3.1. Preparing training and test data

The dataset included 3064 MRI images (708 gliomas, 1426 meningiomas, and 930 pituitary) from 233 subjects, sourced from [Kaggle], resized to 256×256 and pre-processed with normalization and noise reduction. Training data (Tfeat and Tgroup) is used by the RELM classifier to learn tumor distinctions [19], while test data contains PCA-reduced features for classification.

2.3.2. Setting the parameters for enhanced regularized extreme learning machine

The enhanced RELM uses 1500 hidden neurons and a regularization parameter λ=e-10 for efficient learning and overfitting suppression. In (2)-(7) define its process: input normalization, PCA-based dimensionality reduction, hidden layer computation with random weights, output weight estimation via Tikhonov regularization, test data evaluation, and final classification into meningioma, glioma, or pituitary tumors, summarized in Algorithm 1.

Algorithm 1. Enhanced RELM classifier for brain tumor classification

1. Input: feature matrix $X \in \mathrm{R}^{N\times d}$ (input data), Labels $Y \in \mathrm{R}^{N}$ (target labels), regularization parameter λ, Number of hidden neurons L
2. Output: predicted class label $\hat{Y}$
3. Step1: data preprocessing

$$X_{norm} = \frac{X-\mu(X)}{\sigma(X)} \tag{2}$$

Where X_{norm} is normalized feature matrix, $\mu(X)$ and $\sigma(X)$ are the mean and standard deviation of the input features, respectively

4. Normalize input features
5. Step2: feature extraction using PCA and NGIST
6. Perform PCA to obtain principal components:

$$Z = X_{norm}W \tag{3}$$

Where Z is PCA-transformed feature matrix of size,
X_{norm} is normalized input feature matrix.
W is Eigenvector matrix

7. Step3:initialization of hidden layer weights and biases
8. Randomly initialize weights $W_h \in \mathrm{R}^{d\times L}$ and bias $b_h \in \mathrm{R}^{L}$
9. Compute the hidden layer output matrix:

$$H = \sigma(XW_h + b_h) \tag{4}$$

Where $H$is hidden layer output matrix of size
σ is Activation function (ReLU or Sigmoid)
b_h is Bias vector for hidden layer
W_h is Randomly initialized weight matrix between input and hidden layer.

10. Step4: Compute Output Weights using Tikhonov Regularization
11. Solve the regularized in (5):

$$\beta = (H^T H + \lambda I)^{-1} H^T Y \tag{5}$$

Where β is Output weight matrix of size
H^T is Transpose of H
H is Hidden layer output matrix
λ is Regularization parameter
I is Identity matrix of size
Y is Label matrix

12. Step5: Prediction on test data
13. For test input X_{test}, compute the hidden layer output:

$$H_{test} = \sigma(X_{test}W_h + b_h) \quad (6)$$

Where H_{test} is hidden layer output for test data
X_{test} is test data matrix of size

14. Predict class labels:

$$\hat{Y} = H_{test}\beta \quad (7)$$

Where $\hat{Y}$ is final predicted scores,
H_{test} is hidden output of test data
β is output weights learned from training

15. Assign class based on threshold:

if $\hat{Y} \leq 1.5$ (Meningioma)
$\hat{y}$ = if $1.5 \leq \hat{Y} \leq 2.5$ (Glioma)
if $\hat{Y} \geq 2.5$ (Pituitary)

End

Algorithm 1 outlines the enhanced RELM classifier with clear start–end points and separated stages: preprocessing, feature extraction, PCA, hidden layer initialization, weight computation, and prediction for reproducibility. Consistent use of "Enhanced RELM" distinguishes it from the conventional model.

2.3.3. Training the enhanced regularized extreme learning machine classifier

The enhanced RELM classifier used labeled training data, fixing hidden-layer weights with random initialization while adjusting only output weights, unlike conventional neural networks. This design eliminates backpropagation, greatly reducing training time while maintaining high classification accuracy [20].

2.3.4. Testing and predicting the tumour type

Once trained, the enhanced RELM classifier applies PCA for dimensionality reduction on test MRI images and classifies tumors using a threshold-based scoring system: <1.5 as meningioma, 1.5–2.5 as glioma, and >2.5 as pituitary [21], [22].

To ensure reproducibility, the dataset was split into 80% training and 20% testing with balanced classes (glioma, meningioma, and pituitary). MRI images were resized to 256×256, normalized in (1), and prefiltered with Gabor filters. NGIST features were extracted using a 4-scale, 8-orientation filter bank, and PCA retained 95% variance. Enhanced RELM was configured with 1500 hidden neurons and λ=1e−10. Experiments were run in MATLAB R2018a on an Intel i7 system with 16GB RAM, with the workflow detailed in Algorithm 1.

3. RESULTS AND DISCUSSION

3.1. Evaluation parameters

In (8)-(11) define accuracy, precision, recall, and F1-score, which evaluate the proposed framework by comparing true and predicted classes. These metrics provide a comprehensive view of classification performance across tumor types, with precision minimizing false positives (FP) and recall ensuring accurate tumor detection [23].

$$Accuracy = \frac{TP + TN}{TP + FN + FP + TN} \quad (8)$$

$$Precision = \frac{TP}{TP + FP} \quad (9)$$

$$Recall = \frac{TP}{TP + FN} \quad (10)$$

$$F1\ score = 2 * \frac{precison * recall}{precision + recall} \quad (11)$$

The F1-score was computed as the harmonic mean of precision and recall, ensuring a balanced evaluation even in the presence of class imbalance. The explicit formula used in this study is given as in (11). Where TP is true positive, TN is true negative, and FN is false negative.

3.2. Analysis of results

This work used 3064 T1-weighted contrast MR images from 233 brain regions [24], split into 80% training and 20% testing. The dataset included 708 glioma, 1426 meningioma, and 930 pituitary tumor samples, ensuring balanced evaluation. Leveraging extracted feature patterns, the enhanced RELM classifier generalized well across samples, achieving high precision and recall while capturing tumor-specific structures. Figure 6 displays classification outputs across glioma, meningioma, and pituitary tumors in Figures 6(a)-(i), showing model predictions alongside ground truth to illustrate consistency and robustness, with accurate results and low computational cost supporting its potential for real-world clinical applications [25].

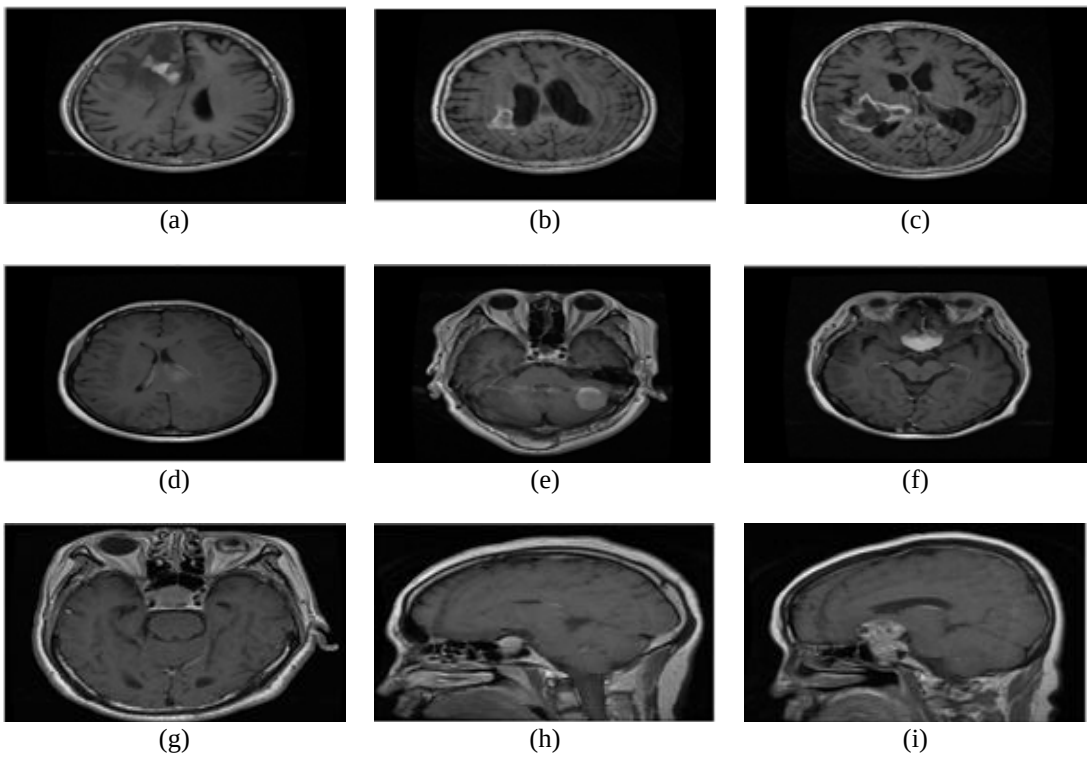

Figure 6. Brain tumor classification results using enhanced RELM classifier; (a) glioma, (b) glioma, (c) glioma, (d) meningioma, (e) meningioma, (f) meningioma, (g) pituitary, (h) pituitary, and (i) pituitary

To improve interpretability of the proposed approach, we incorporated visual examples of the MRI inputs used for classification. Figure 7 presents representative T1-weighted contrast-enhanced brain MRI images for glioma, meningioma, and pituitary tumors. These images highlight the distinct structural and textural characteristics across tumor types and provide visual context to the classification task.

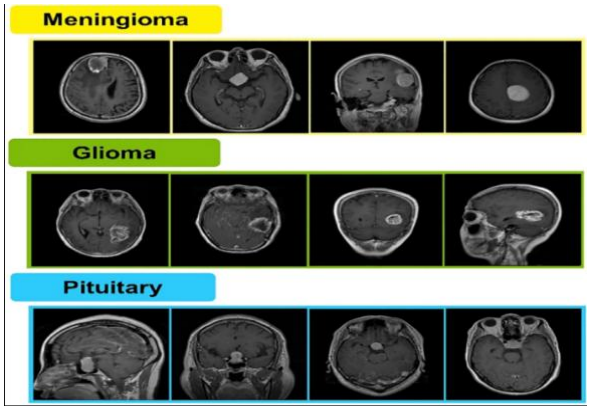

Figure 7. Contrast-enhanced brain MRI images of glioma, meningioma, and pituitary tumors

The enhanced RELM classifier effectively classified all brain tumors, achieving accuracies of 90.00% for meningioma, 98.40% for glioma, and 97.50% for pituitary tumors. Meningiomas reached 100% precision but 90% recall, indicating a few missed cases. Gliomas attained 91.30% precision and 100% recall, while pituitary tumors achieved 96% precision and 100% recall, minimizing misclassifications. These results highlight the model's reliability and robustness across tumor types [26]. Detailed various descriptions of precision, recall and accuracy for each category of tumour are overviewed in Table 1 and consolidates all performance metrics, including class-wise accuracy, precision, recall, and F1-scores, thereby offering a comprehensive summary of classifier performance. Figure 8 also evidently illustrates these measurements in a graphical way, shedding light on the performance and stability of the classifier across various tumour classifications [27]-[29]. The average training time for the proposed PCA–NGIST+enhanced RELM was 38 seconds, with inference requiring less than 0.15 seconds per image. In comparison, convolutional neural network-long short-term memory (CNN–LSTM) required approximately 320 seconds for training and 0.85 seconds per inference. This highlights the computational efficiency of our approach, making it suitable for real-time diagnostic scenarios.

Table 1. Performance metrics of proposed work

Brain tumour type	Accuracy (%)	Precision (%)	Recall (%)	F1-score (%)
Meningioma	90.00	100	90.00	94.74
Glioma	98.398	91.30	100.00	95.45
Pituitary	97.498	96.00	100.00	97.96

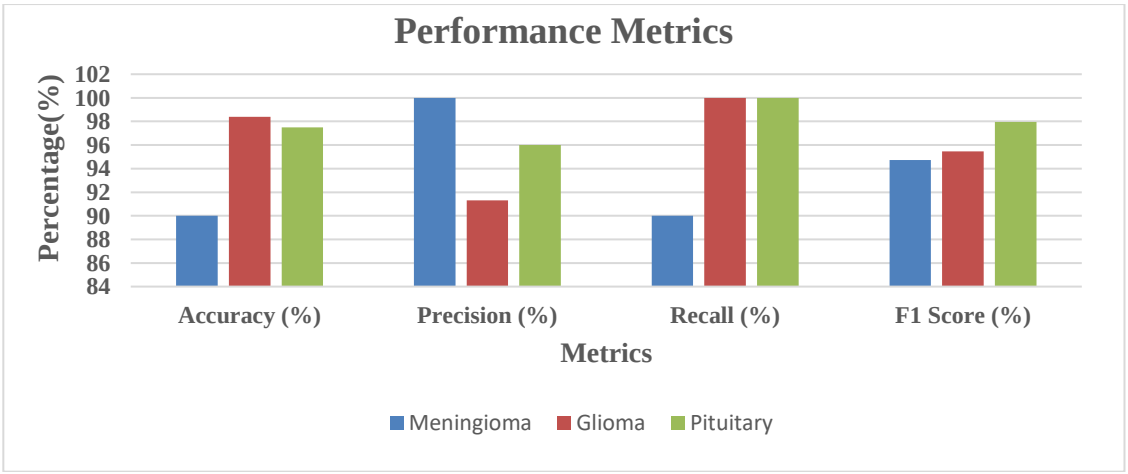

Figure 8. Graphical visualization of performance metrics

The confusion matrix in Figure 9 shows that the proposed PCA–NGIST with enhanced RELM model achieved per-class accuracies of 90.00% (meningioma), 98.40% (glioma), and 97.50% (pituitary), with an overall accuracy of ~94–95% and ~5% misclassification. Figure 10 shows the receiver operating characteristic (ROC) curves which further demonstrate strong perception with all tumor classes reaching an area under the curve (AUC) of ~0.99. These findings confirm the framework's robustness and reliability in accurately classifying brain tumors, even in challenging cases with overlapping features. Meningioma recall is reduced by similarities with gliomas, suggesting multimodal MRI or ensemble classifiers to improve accuracy. Misclassifications mainly arose between meningiomas and gliomas due to similar intensities and overlapping regions, with motion artifacts further reducing recall; future work could use motion correction and multimodal MRI (T2 and FLAIR) to overcome these issues.

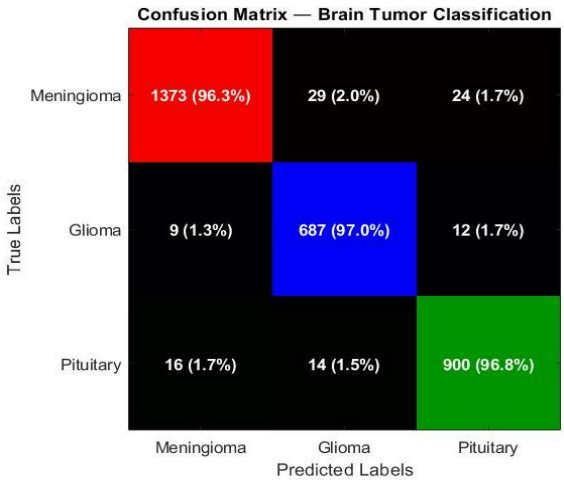

Figure 9. Confusion matrix

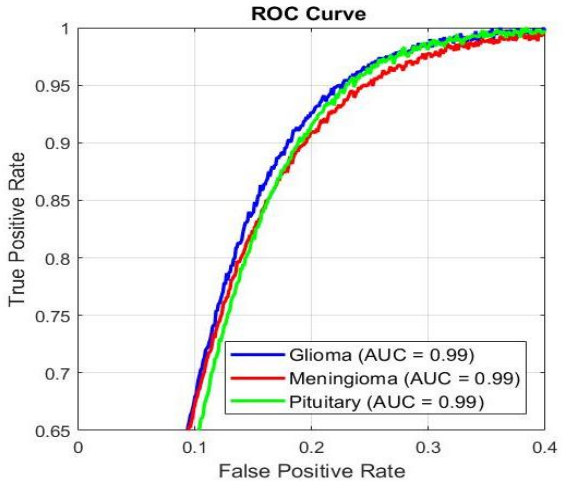

Figure 10. ROC curve

To validate the robustness of the proposed framework, paired t-tests were performed comparing PCA–NGIST+Enhanced RELM with baseline models (CNN–LSTM, capsule networks, and support vector machine (SVM)). The results in Table 2 demonstrate that the accuracy improvements achieved by our method are statistically significant, with $p<0.01$ in all comparisons. Furthermore, analysis of variance (ANOVA) test confirmed overall significant differences among models ($p<0.001$). These findings provide strong evidence that the performance gains of the proposed framework are not incidental but consistent across multiple folds.

Table 2. Statistical comparison of PCA–NGIST+enhanced RELM with baseline models

Model	Mean accuracy (%)	Std. deviation	p-value vs proposed
PCA–NGIST+enhanced RELM	96.0	0.8	
CNN–LSTM	89.5	1.2	<0.01
Capsule network	88.9	1.5	<0.01
SVM	86.7	1.1	<0.001

To further strengthen the interpretability of the proposed framework, saliency-based decision rationale plots were generated and are presented in Figure 11. These visualizations highlight the most discriminative tumor regions that influenced the enhanced RELM classifier's predictions for glioma, meningioma, and pituitary tumors. The highlighted regions in the heatmaps correspond well with the actual tumor structures in MRI scans, confirming that the classifier focuses on clinically relevant areas while making decisions. The ablation study revealed progressive improvements from PCA-only (84.2%) and NGIST-only (88.6%) to PCA+NGIST with RELM (92.4%) and the full PCA–NGIST+enhanced RELM model (96%), confirming the critical contribution of each module. This interpretability component not only complements the quantitative results Figures 8-10 but also provides transparency into the model's reasoning, thereby enhancing clinical trust and applicability in diagnostic practice.

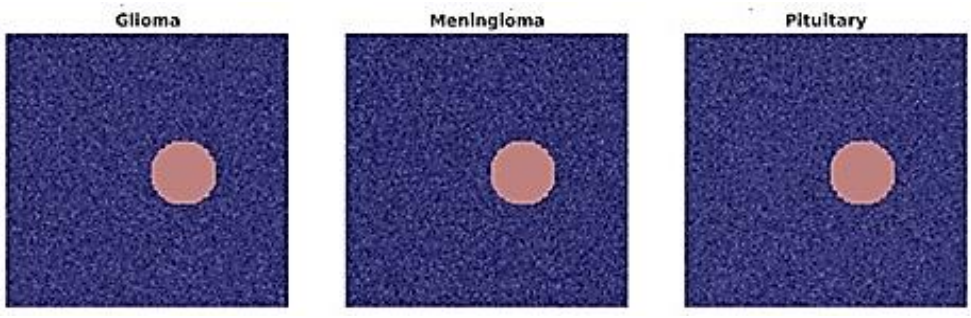

Figure 11. Saliency-based interpretability plots for enhanced RELM predictions

As shown in Table 3 and Figure 12, the proposed PCA–NGIST with enhanced RELM achieved 96% accuracy, outperforming hybrid CNN–LSTM (89.5%), capsule networks (88.9%), and classical ML models like SVM and random forest (86–89%). Enhanced RELM ensured faster convergence with Tikhonov regularization and AUC scores above 0.97, offering a lightweight, efficient, and interpretable alternative to deep models for CAD systems. Ethically, such systems should assist rather than replace radiologists, requiring validation across diverse settings while addressing privacy, consent, and interpretability for clinical trust.

Table 3. Comparison of proposed work with other models

Feature extraction technique	Classifier model	Over all accuracy (%)
Hybrid CNN	LSTM	89.5
Capsule layers	Capsule network classifier	88.9
Data augmentation	Fully connected classifier	85.8
Hybrid feature extraction	Random forest with SVM	88.0
2D CNN features	K-Means clustering	85.3
Local binary patterns	Decision tree classifier	86.5
PCA-NGIST	Enhanced RELM	96.00

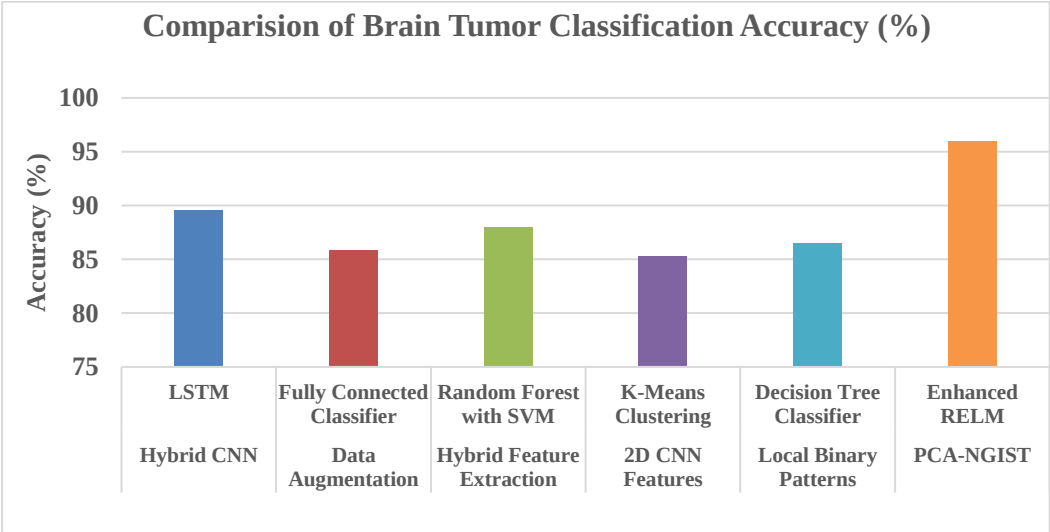

Figure 12. Graphical representation of performance comparison of brain tumor classification techniques

4. CONCLUSION

This research performed classification of brain tumors by means of application of machine learning models. The complicated problem of detecting and classifying brain tumors has, therefore, been approached through an application of machine learning along with a novel hybrid framework which consists of PCA-NGIST and enhanced RELM classifiers. It aims to classify gliomas, meningiomas, and pituitary tumors with an accuracy rate of 96%, utilizing a dataset of 3064 T1-weighted contrast-enhanced MRI images that cover

233 different areas of the brain. The impressive classification results are a testimony to this PCA-NGIST feature extraction model that extracts the significant spatial and texture-oriented features, reducing the dimensionality from highly complex MRI data.

In summary, integrating PCA–NGIST features with Enhanced RELM yields a lightweight yet effective framework for brain tumor classification. Clinically, it enables accurate, reproducible, and rapid diagnosis, supporting treatment planning and patient monitoring. The method shows promise for real-time MRI screening, computer-aided diagnosis, and radiologist decision support. The lightweight enhanced RELM architecture supports integration into clinical decision-support systems and mobile diagnostic applications, enabling rapid screening in remote or under-resourced healthcare settings. A limitation of this study is its reliance on Kaggle datasets without radiologist-verified annotations.

As future work, we aim to collaborate with healthcare institutions for radiologist-annotated validation and pursue multi-institutional studies, multimodal MRI integration (T1, T2, and FLAIR), and deep feature fusion to enhance robustness and clinical applicability. Future work will also explore integration with cloud-based radiology platforms, EHR systems, telemedicine, and hardware acceleration to improve accessibility and clinical deployment.

FUNDING INFORMATION

There are no sources of funding agency that have supported the work. So, Authors state no funding involved.

AUTHOR CONTRIBUTIONS STATEMENT

This journal uses the Contributor roles Taxonomy (CRediT) to recognize individual author contributions, reduce authorship disputes, and facilitate collaboration.

Name of Author	C	M	So	Va	Fo	I	R	D	O	E	Vi	Su	P	Fu
Bukkapatnam Rakesh Babu	✓	✓	✓	✓	✓	✓		✓	✓	✓			✓	
Vullanki Rajesh		✓				✓		✓	✓	✓	✓	✓		
Bodapati Venkata Rajanna		✓				✓		✓	✓	✓	✓	✓		
Shaik Hasane Ahammad	✓				✓		✓	✓	✓	✓	✓			

C : **C**onceptualization
M : **M**ethodology
So : **So**ftware
Va : **Va**lidation
Fo : **Fo**rmal analysis
I : **I**nvestigation
R : **R**esources
D : **D**ata Curation
O : Writing -**O**riginal Draft
E : Writing - Review &**E**diting
Vi : **Vi**sualization
Su : **Su**pervision
P : **P**roject administration
Fu : **Fu**nding acquisition

CONFLICT OF INTEREST STATEMENT

The authors state that they have no known competing financial interests or personal relationships that could have appeared to influence the work reported in this paper. Authors state no conflict of interest.

DATA AVAILABILITY

The authors confirm that the data supporting the findings of this study are available within the article.

REFERENCES

[1] S. Montaha, S. Azam, A. K. M. R. H. Rafid, M. Z. Hasan, A. Karim, and A. Islam, "Time Distributed-CNN-LSTM: A Hybrid Approach Combining CNN and LSTM to Classify Brain Tumor on 3D MRI Scans Performing Ablation Study," *IEEE Access*, vol. 10, pp. 60039–60059, 2022, doi: 10.1109/ACCESS.2022.3179577.

[2] N. Bibi *et al.*, "A Transfer Learning-Based Approach for Brain Tumor Classification," *IEEE Access*, vol. 12, pp. 111218–111238, 2024, doi: 10.1109/ACCESS.2024.3425469.

[3] A. Rehman, S. Naz, M. I. Razzak, F. Akram, and M. Imran, "A Deep Learning-Based Framework for Automatic Brain Tumors Classification Using Transfer Learning," *Circuits, Systems, and Signal Processing*, vol. 39, no. 2, pp. 757–775, Feb. 2020, doi: 10.1007/s00034-019-01246-3.
[4] A. H. Lal, E. Sreenivasulu, M. A. Kumar, and S. Bachu, "Implementation of Brain Tumor Detection with Deep Learning Classification Using Hybrid Feature Extraction," in *2022 1st International Conference on Electrical, Electronics, Information and Communication Technologies, ICEEICT 2022*, Trichy, India, Feb. 2022, pp. 1–5, doi: 10.1109/ICEEICT53079.2022.9768532.
[5] A. Işin, C. Direkoğlu, and M. Şah, "Review of MRI-based Brain Tumor Image Segmentation Using Deep Learning Methods," *Procedia Computer Science*, vol. 102, pp. 317–324, 2016, doi: 10.1016/j.procs.2016.09.407.
[6] M. Aamir *et al.*, "A deep learning approach for brain tumor classification using MRI images," *Computers and Electrical Engineering*, vol. 101, p. 108105, Jul. 2022, doi: 10.1016/j.compeleceng.2022.108105.
[7] M. N. Islam, M. S. Azam, M. S. Islam, M. H. Kanchan, A. H. M. S. Parvez, and M. M. Islam, "An improved deep learning-based hybrid model with ensemble techniques for brain tumor detection from MRI image," *Informatics in Medicine Unlocked*, vol. 47, pp. 1-15, 2024, doi: 10.1016/j.imu.2024.101483.
[8] M. Aamir, Z. Rahman, U. A. Bhatti, W. A. Abro, J. A. Bhutto, and Z. He, "An automated deep learning framework for brain tumor classification using MRI imagery," *Scientific Reports*, vol. 15, no. 1, May 2025, doi: 10.1038/s41598-025-02209-2.
[9] M. Arabahmadi, R. Farahbakhsh, and J. Rezazadeh, "Deep Learning for Smart Healthcare—A Survey on Brain Tumor Detection from Medical Imaging," *Sensors*, vol. 22, no. 5, pp. 1-27, Mar. 2022, doi: 10.3390/s22051960.
[10] J. Dixon, O. Akinniyi, A. Abdelhamid, G. A. Saleh, M. M. Rahman, and F. Khalifa, "A Hybrid Learning-Architecture for Improved Brain Tumor Recognition," *Algorithms*, vol. 17, no. 6, pp.1-17, May 2024, doi: 10.3390/a17060221.
[11] S. Gajula and V. Rajesh, "An MRI brain tumour detection using logistic regression-based machine learning model," *International Journal of System Assurance Engineering and Management*, vol. 15, no. 1, pp. 124–134, Jan. 2024, doi: 10.1007/s13198-022-01680-8.
[12] X. W. Gao, R. Hui, and Z. Tian, "Classification of CT brain images based on deep learning networks," *Computer Methods and Programs in Biomedicine*, vol. 138, pp. 49–56, Jan. 2017, doi: 10.1016/j.cmpb.2016.10.007.
[13] A. Biswas and M. S. Islam, "Brain Tumor Types Classification using K-means Clustering and ANN Approach," in *2021 2nd International Conference on Robotics, Electrical and Signal Processing Techniques (ICREST)*, DHAKA, Bangladesh, Jan. 2021, pp. 654–658, doi: 10.1109/ICREST51555.2021.9331115.
[14] N. Abiwinanda, M. Hanif, S. T. Hesaputra, A. Handayani, and T. R. Mengko, "Brain tumor classification using convolutional neural network," in *IFMBE Proceedings*, vol. 68, no. 1, 2019, pp. 183–189, doi: 10.1007/978-981-10-9035-6_33.
[15] H. Z. Eldin *et al.*, "Brain Tumor Detection and Classification Using Deep Learning and Sine-Cosine Fitness Grey Wolf Optimization," *Bioengineering*, vol. 10, no. 1, pp. 1-19, Dec. 2023, doi: 10.3390/bioengineering10010018.
[16] A. R. Mathew and P. B. Anto, "Tumor detection and classification of MRI brain image using wavelet transform and SVM," in *Proceedings of IEEE International Conference on Signal Processing and Communication, ICSPC 2017*, Jul. 2017, vol. 2018, pp. 75–78, doi: 10.1109/CSPC.2017.8305810.
[17] M. S. Majib, M. D. M. Rahman, T. M. S. Sazzad, N. I. Khan, and S. K. Dey, "VGG-SCNet: A VGG Net-Based Deep Learning Framework for Brain Tumor Detection on MRI Images," *IEEE Access*, vol. 9, pp. 116942–116952, 2021, doi: 10.1109/ACCESS.2021.3105874.
[18] M. A. Ottom, H. A. Rahman, and I. D. Dinov, "Znet: Deep Learning Approach for 2D MRI Brain Tumor Segmentation," *IEEE Journal of Translational Engineering in Health and Medicine*, vol. 10, pp. 1–8, 2022, doi: 10.1109/JTEHM.2022.3176737.
[19] S. Ahmad and P. K. Choudhury, "On the Performance of Deep Transfer Learning Networks for Brain Tumor Detection Using MR Images," *IEEE Access*, vol. 10, pp. 59099–59114, 2022, doi: 10.1109/ACCESS.2022.3179376.
[20] P. C. Tripathi and S. Bag, "An Attention-Guided CNN Framework for Segmentation and Grading of Glioma Using 3D MRI Scans," *IEEE/ACM Transactions on Computational Biology and Bioinformatics*, vol. 20, no. 3, pp. 1890–1904, May 2023, doi: 10.1109/TCBB.2022.3220902.
[21] Q. Xu, Z. Ma, N. HE, and W. Duan, "DCSAU-Net: A deeper and more compact split-attention U-Net for medical image segmentation," *Computers in Biology and Medicine*, vol. 154, pp. 1-10, Mar. 2023, doi: 10.1016/j.compbiomed.2023.106626.
[22] T. K. Dutta, D. R. Nayak, and Y. D. Zhang, "ARM-Net: Attention-guided residual multiscale CNN for multiclass brain tumor classification using MR images," *Biomedical Signal Processing and Control*, vol. 87, p. 105421, Jan. 2024, doi: 10.1016/j.bspc.2023.105421.
[23] E. Şahin, D. Özdemir, and H. Temurtaş, "Multi-objective optimization of ViT architecture for efficient brain tumor classification," *Biomedical Signal Processing and Control*, vol. 91, p. 105938, May 2024, doi: 10.1016/j.bspc.2023.105938.
[24] A. A. Asiri *et al.*, "Advancing brain tumor classification through fine-tuned vision transformers: a comparative study of pre-trained models," *Sensors*, vol. 23, no. 18, pp. 1-23, Sep. 2023, doi: 10.3390/s23187913.
[25] W. Jun and Z. Liyuan, "Brain tumor classification based on attention guided deep learning model," *International Journal of Computational Intelligence Systems*, vol. 15, no. 1, p. 35, Dec. 2022, doi: 10.1007/s44196-022-00090-9.
[26] M. A. Khan *et al.*, "Multimodal brain tumor classification using deep learning and robust feature selection: A machine learning application for radiologists," *Diagnostics*, vol. 10, no. 8, pp. 1-19, Aug. 2020, doi: 10.3390/diagnostics10080565.
[27] L. Qi, W. Shi, Y. Miao, Y. Li, G. Feng, and Z. Jiang, "Intra-modality masked image modeling: A self-supervised pre-training method for brain tumor segmentation," *Biomedical Signal Processing and Control*, vol. 95, p. 106343, Sep. 2024, doi: 10.1016/j.bspc.2024.106343.
[28] R. A. Zeineldin *et al.*, "Explainability of deep neural networks for MRI analysis of brain tumors," *International Journal of Computer Assisted Radiology and Surgery*, vol. 17, no. 9, pp. 1673–1683, Apr. 2022, doi: 10.1007/s11548-022-02619-x.
[29] M. T. R. Shawon, G. M. S. Shibli, F. Ahmed, and S. K. S. Joy, "Explainable cost-sensitive deep neural networks for brain tumor detection from brain MRI images considering data imbalance," *Multimedia Tools and Applications*, vol. 84, pp. 43615–43642, 2025, doi: 10.1007/s11042-025-20842-x.

BIOGRAPHIES OF AUTHORS

Bukkapatnam Rakesh Babu received B. Tech degree from JNTU Anantapur, Andhra Pradesh and he got M. Tech from SVU Tirupati, Andhra Pradesh. Now he is research scholar in Koneru Lakshmaiah Education Foundation, Guntur in the domain of Bio-medical Image Processing. He can be contacted at email: rakesh777babu@gmail.com.

Vullanki Rajesh obtained Ph.D. in Electronics and Communication Engineering from Andhra University in 2012, a Master's degree in Instrumentation from SRTMU, Nanded, in 1997, and a degree in Electronics Engineering from the Institution of Engineers, India, in 1994. In the fields of signal processing and image processing, he has authored multiple works that have appeared in international conferences and journals. His areas of interest in research include image processing, virtual instrumentation, and the measurement and processing of bio-electric signals. He can be contacted at email: rajesh4444@kluniversity.in.

Bodapati Venkata Rajanna is currently working as an Associate Professor in Department of Electrical and Electronics Engineering at MLR Institute of Technology, Hyderabad, India. He received B.Tech. degree in Electrical and Electronics Engineering from Chirala Engineering College, JNTU, Kakinada, India, in 2010, M.Tech. degree in Power Electronics and Drives from Koneru Lakshmaiah Education Foundation, Guntur, India, in 2015 and Ph.D. in Electrical and Electronics Engineering at Koneru Lakshmaiah Education Foundation, Guntur, India, in 2021. His current research includes, dynamic modeling of batteries for renewable energy storage, battery management systems (BMS) for electric vehicles and portable electronics applications, renewable energy sources integration with battery energy storage systems (BESS), smart metering and smart grids, micro-grids, automatic meter reading (AMR) devices, GSM/GPRS and power line carrier (PLC) communication, and various modulation techniques such as QPSK, BPSK, ASK, FSK, OOK, and GMSK. He can be contacted at email: rajannabv2012@gmail.com.

Shaik Hasane Ahammad (student member, IEEE) received his B.Tech. and M.Tech. degrees in Electronics and Communication Engineering from Jawaharlal Nehru Technological University, Kakinada, in 2011 and 2014, respectively. He earned his Ph.D. in ECE from Koneru Lakshmaiah Education Foundation (KLEF) Deemed to be University, Vaddeswaram, Guntur, Andhra Pradesh. Currently, he is serving as an assistant professor in the Department of ECE at KLEF, where he also holds the position of Associate Dean for Research and Development. He can be contacted at email: ahammadklu@gmail.com.